FEBS Letters

FEBS PRESS science publishing by scientists

Targeting RIPK3 oligomerization blocks necroptosis without inducing apoptosis

Wenjuan Li[1,2], Hengxiao Ni[1,2], Shaofeng Wu[1,2,3], Shang Han[1,2,3], Chang'an Chen[1,2], Li Li[1,2,3], Yunzhan Li[1,2,3], Fu Gui[1,2,3], Jiahuai Han[1,2] and Xianming Deng[1,2,3]

1 School of Life Sciences, Xiamen University, Xiamen, China
2 Cancer Research Center of Xiamen University, Xiamen, China
3 State-Province Joint Engineering Laboratory of Targeted Drugs from Natural Products, Xiamen University, Xiamen, China

Correspondence
X. Deng and J. Han, School of Life Sciences, Xiamen University, No. 4221-120 South Xiang'an Road, Xiang'an District, Xiamen, Fujian 361102, China
Tel: +86 592 2184180; +86 592 2189390
E-mails: xmdeng@xmu.edu.cn; jhan@xmu.edu.cn

(Received 20 December 2019, revised 25 April 2020, accepted 27 April 2020, available online 1 June 2020)

doi:10.1002/1873-3468.13812

Edited by Barry Halliwell

Receptor-interacting serine/threonine-protein kinase 3 (RIPK3) is a central protein in necroptosis with great potential as a target for treating necroptosis-associated diseases, such as Crohn's disease. However, blockade of RIPK3 kinase activity leads to unexpected RIPK3-initiated apoptosis. Herein, we found that PP2, a known SRC inhibitor, inhibits TNF-α-induced necroptosis without initiating apoptosis. Further investigation showed that PP2 acts as an inhibitor of not only SRC but also RIPK3. PP2 does not disturb the integrity of the RIPK1–RIPK3–mixed lineage kinase domain-like pseudokinase (MLKL) necroptosome or the autophosphorylation of RIPK3 at T231/S232 but disrupts RIPK3 oligomerization, thereby impairing the phosphorylation and oligomerization of MLKL. These results demonstrate the essential role of RIPK3 oligomerization in necroptosis and suggest a potential RIPK3 oligomerization-targeting strategy for therapeutic development.

Keywords: apoptosis; necroptosis; oligomerization; phosphorylation; RIPK3

Necroptosis is involved in the processes of multiple diseases, including inflammatory bowel diseases, such as Crohn's disease [1] and atherosclerosis [2]. It also causes severe transplantation rejection and reduces transplant survival [3]. Upon stimulation with tumor necrosis factor-α (TNF-α), receptor-interacting serine/threonine-protein kinase 1 (RIPK1) has been widely shown to be activated and recruit RIPK3, followed by RIPK3 dimerization or oligomerization, which leads to RIPK3 autophosphorylation at T231/S232 [4]. Phosphorylated RIPK3 recruits and phosphorylates mixed lineage kinase domain-like pseudokinase (MLKL) at S345 [5]. Phosphorylated MLKL is prone to form disulfide bond-linked oligomers on the plasma membrane, ultimately causing high intracellular osmotic pressure that leads to necroptosis [6–8]. Targeting this pathway using small molecules holds great promise for the development of therapeutics against necroptosis-related diseases.

RIPK3, an essential hub in necroptosis, consists of a receptor-interacting serine/threonine-protein homotypic interaction motif (RHIM) domain and a kinase domain. The RHIM domain is responsible for protein–protein interactions among members of the RHIM family, such as RIPK1, DNA-dependent activator of IFN regulatory factors, and Toll-like receptor adaptor molecule 1. The ability of RIPK3 deficiency to impair necroptosis has heightened interest in the

Abbreviations
FKBP, FK506-binding protein; RHIM, receptor-interacting serine/threonine-protein homotypic interaction motif; RIPK3, receptor-interacting serine/threonine-protein kinase 3; TNF-α, tumor necrosis factor-α.

therapeutic potential of small-molecule inhibitors that target RIPK3 kinase activity. However, impairment of kinase activity seems to turn RIPK3 from a necroptosis inducer into an apoptosis inducer, since both a genetic kinase-dead RIPK3 mutant, D161N RIPK3 [9], and the RIPK3 kinase activity inhibitor GSK872 [10] led to unexpected severe side effects by initiating apoptosis. Interestingly, the other RIPK3 mutations K51A, D161G (two of the catalytic triad residues Lys51/Glu61/Asp161), and D143N (on the catalytic loop) [10] have not shown such side effects. This finding prompted us to search for small molecules that can control RIPK3-mediated necroptosis without inducing RIPK3-mediated apoptosis and uncover their detailed molecular mechanism.

Herein, we found that 1-(tert-butyl)-3-(4-chlorophenyl)-1H-pyrazolo[3,4-d]pyrimidin-4-amine (also known as PP2), a reported SRC inhibitor, blocked TNF-α-induced necroptosis without initiating apoptosis, which appeared to be independent of PP2-mediated inhibition of SRC. Further investigation revealed that PP2 disrupted RIPK3 oligomerization without affecting its autophosphorylation. Our results elucidate the critical role of RIPK3 oligomerization in necroptosis, which suggests a potential RIPK3 oligomerization-targeting strategy for necroptosis regulation without apoptotic side effects.

Materials and methods

Cell lines and cell culture

L929 mouse fibrosarcoma cells were obtained from ATCC (Manassas, VA, USA) and maintained in DMEM supplemented with 10% fetal bovine serum, 4 mM L-glutamine, 100 IU penicillin, and 100 mg·mL^{-1} streptomycin at 37 °C in a humidified incubator containing 5% CO_2. Genetic knockout L929 cell lines (RIPK1-knockout, RIPK3-knockout, and MLKL-knockout cells) were generated by the CRISPR/Cas9 method as described in previous works [4]. The target sites for Fyn were designed as 'TGGATACTATATCACAACGC'. The knockout cells were verified by sequencing the targeted loci.

Reagents and antibodies

PP2 (cat. #HY-13805) was purchased from MedChemExpress (Trenton, NJ, USA). AP21967, identical to A/C heterodimerizer (cat. #635055), was obtained from Takara Biomedical Technology (Beijing, China). Gallein (cat. #371708), Src-i-1 (cat. #S2075), the lymphocyte-specific protein tyrosine kinase (Lck) inhibitor 7-cyclopentyl-5-(4-phenoxypheny)-7H-pyrrolo[2,3d]pyrimidin-4-ylamine (cat. #C88634), Z-VAD-FMK (cat. #V116), and 4-hydroxytamoxifen (4-OHT, cat. #H7904) were purchased from Sigma (St. Louis, MO, USA). Mouse anti-HA (F-7) (cat. #sc-7392) and mouse anti-GAPDH (6C5) (cat. #sc-32233) antibodies were purchased from Santa Cruz Biotechnology, Inc. (Dallas, TX, USA). Mouse anti-HA agarose (cat. #A2095) and mouse anti-Flag (M2) (cat. #F1804) antibodies were purchased from Sigma. Anti-mRIPK3 was raised in rabbits using *Escherichia coli*-expressed GST-mRIPK3 (amino acids 287–387).

Plasmid construction

Full-length RIPK1, mouse RIPK3, MLKL, and related genes were amplified from an in-house cDNA library. Plasmid construction was described in detail in our previous study [11].

Lentivirus preparation and infection

Lentivirus preparation and infection were performed as previously described [4]. HEK293T cells were cotransfected with pBOB constructs and lentivirus packaging plasmids (pMDL, pREV, and pVSVG) by calcium phosphate precipitation. The medium was changed after 16 h. Lentivirus-containing supernatants were collected 32 h later and used for infection in the presence of 10 μg·mL^{-1} Polybrene.

Cell death assay

Cell viability was analyzed using a CellTiter-Glo Luminescent Cell Viability Assay according to the manufacturer's instructions (Promega, G9241, Madison, WI, USA). In brief, 10^5 cells were seeded in 96-well plates (Nunc 152028). After treatment, an equal volume of CellTiter-Glo reagent was added to the cell culture medium, followed by equilibration at room temperature for 30 min. Then, the plates were shaken for 5 min and incubated at room temperature for 15 min. Luminescent recording was performed with a POLARstar Omega plate reader (BMG Labtech, Durham, NC, USA). The percentage of cell loss was determined by the percentage of ATP loss. The results are presented as the mean ± SEM.

Immunoprecipitation and western blotting

For Flag immunoprecipitation, cells were washed with ice-cold PBS and lysed in lysis buffer (20 mM Tris/HCl, pH 7.5, 150 mM NaCl, 1 mM Na_2EDTA, 1 mM EGTA, 1% Triton X-100, 2.5 mM sodium pyrophosphate, 1 mM β-glycerophosphate, 1 mM Na_3VO_4) supplemented with Sigma protease inhibitor cocktail. Cell lysates were centrifuged at 20 000 ***g*** for 30 min, and the supernatants were subjected to immunoprecipitation with mouse anti-Flag M2 beads at

4 °C overnight. The beads were then washed three times in lysis buffer the next day, and proteins eluted in 1.2× Laemmli buffer were then analyzed by routine western blotting. Immunoprecipitates and cell lysates were resolved by SDS/PAGE, following which the proteins were transferred onto a polyvinylidene difluoride membrane that was probed with appropriate antibodies. For nonreducing gel analysis, cells were lysed in normal lysis buffer without DTT or β-mercaptoethanol and then applied to a 4–12% gradient SDS/PAGE (Invitrogen, Carlsbad, CA, USA, NP0336BOX).

Results

PP2 delayed TNF-α+zVAD (TZ)-induced necroptosis without inducing apoptosis

Targeting RIPK3 impairs necroptotic cell death. The RIPK3 inhibitor GSK872 (Fig. 1A) potently inhibited TNF-α-induced necroptosis with an EC_{50} of 0.26 μM (Fig. 1B). However, GSK872 treatment led to a substantial dose- and time-dependent increase in apoptosis, but GSK872-induced cell death could be significantly rescued by zVAD, an established caspase inhibitor that prevents apoptosis (Fig. 1C,D). PP2 (Fig. 1A), an SRC inhibitor, also blocked RIPK3-dependent necrosis with an EC_{50} of 1.44 μM (Fig. 1B), which is consistent with our previous study [12]. To our surprise, PP2 did not induce cell death even at a concentration 2–5-fold higher than its EC_{50} value (Fig. 1C,D). Further investigation using an *in vitro* biochemical kinase assay showed that PP2 also inhibited RIPK3 kinase activity with an IC_{50} of 46.5 nM [13] (Fig. 1E). These results prompt us to dissect the molecular mechanism underlying such distinct outcomes of RIPK3 kinase inhibition.

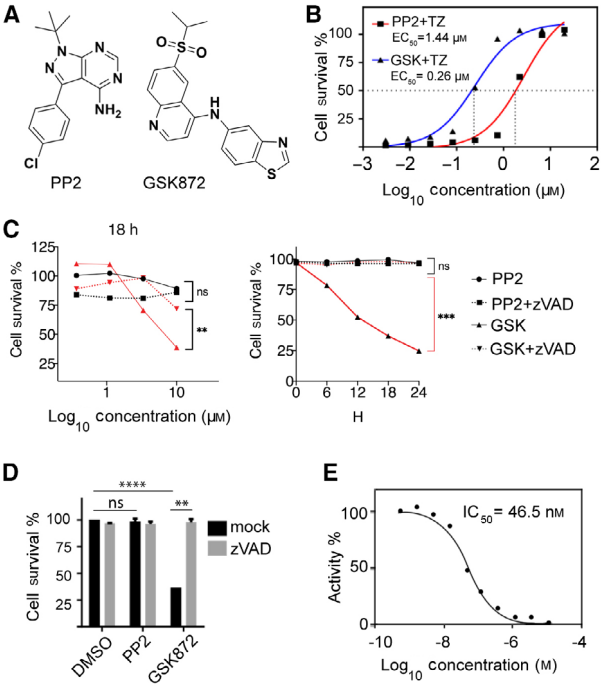

Fig. 1. PP2 attenuates TZ-induced necroptosis without initiating apoptosis. (A) Chemical structures of PP2 and GSK872. (B) The efficiency of PP2- and GSK872-mediated blockade of TNF-α+zVAD (TZ)-induced necroptosis in L929 cells. L929 cells were treated with TNF-α (10 ng·mL^{-1}) and zVAD (20 μM) with PP2 or GSK872 for 4 h as indicated. Cell viability was determined by CellTiter-Glo assay. (C) L929 cells were treated with PP2 or GSK872 at a series of concentrations alone or with zVAD (20 μM) as indicated for 18 h (left). L929 cells were treated with PP2 (10 μM) or GSK872 (10 μM) alone or with zVAD (20 μM) for specific time courses (right). Cell viability was measured by CellTiter-Glo assay. (D) Cellular toxicity was measured by CellTiter-Glo assay after treatment of L929 cells with compounds at a concentration twofold higher than their EC_{50} values for 24 h. (E) The IC_{50} of PP2 against RIPK3 kinase activity was determined using a radiometric biochemical assay (Reaction Biology Corporation, Malvern, PA, USA). ****$P < 0.0001$, extremely significant; **$P < 0.01$, very significant; ns, $P \geq 0.05$, not significant.

PP2 blocked necroptosis by inhibiting RIPK3 independent of the Src family

RIPK3 is considered the key protein in TNF-α-induced necroptosis. Activation of canonical necroptosis includes the formation of a complex containing RIPK1 and RIPK3 and recruitment of the MLKL protein. MLKL phosphorylated by RIPK3 is oligomerized and then translocates to the plasma membrane, ultimately leading to cellular osmotic disruption (Fig. 2A). Our previous study reported that PP2 (Fig. 1A) protected L929 cells from TNF-α-induced necroptosis through inhibition of the Gβγ-Src signaling pathway [12]. To further characterize the detailed mechanism by which PP2 inhibits necroptosis, we used a series of cell lines expressing the RIPK1, RIPK3, and MLKL proteins fused with the hormone-binding domain of the estrogen receptor with the G521R mutation (HBD*) to trace the necroptosis pathway downstream of RIPK1, RIPK3, and MLKL, respectively [11]. HBD* fused with RIPK1-ΔDD, RIPK3 $RHIM^{mut}$, or MLKL formed dimers upon 4-OHT treatment, which led to RIPK1-, RIPK3-, or MLKL-initiated necroptosis directly without the involvement of upstream factors (Fig. 2B). The Gβγ inhibitor gallein and the selective SRC inhibitor SRC-i-1 were also used for comparison. As anticipated, all three inhibitors impaired TNF-α-induced necroptosis in L929 cells, as reported in a previous work [12]. However, they showed different

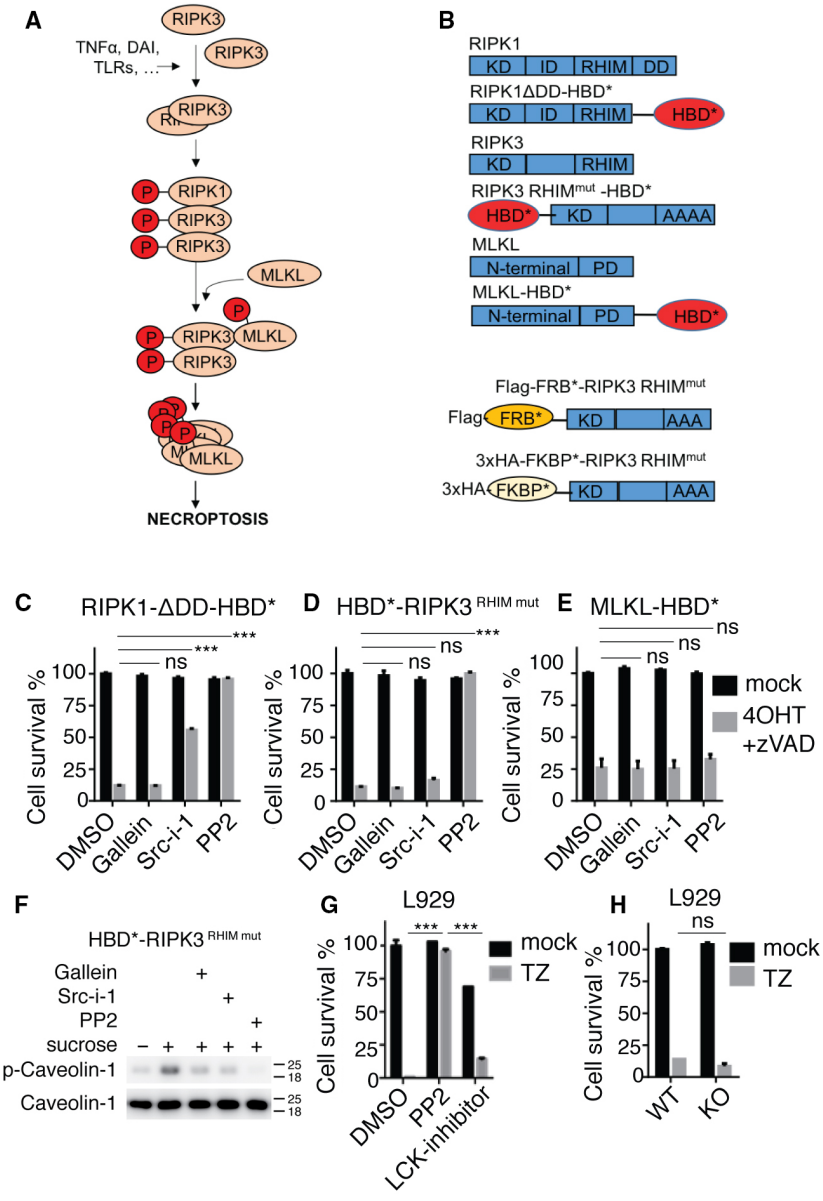

Fig. 2. PP2 serves as a direct RIPK3 inhibitor rather than an SRC inhibitor to block TZ-induced necroptosis. (A) A brief cartoon model showing RIPK3 autophosphorylation and oligomerization, followed by recruitment and phosphorylation of MLKL, resulting in TNF-α-induced necroptosis. (B) Schematic representation of the artificial dimerization system. RHIM^{mut} represents the RIPK3 QIG449–451AAA mutation in the RHIM domain. KD, ID, DD, and PD are abbreviations for the kinase domain, intermediate domain, death domain, and pseudokinase domain, respectively. (C–E) Lentivirus encoding RIPK1ΔDD-HBD* (C), RIPK3-RHIM^{mut}-HBD* (D), or MLKL-HBD* (E) was packaged in HEK293T cells and used to infect RIPK1, RIPK3, and MLKL KO L929 cells, respectively. These reconstituted L929 cells were then treated with 4-OHT (50 nM) and zVAD (20 μM) for 6 h in (C) or 4 h in (D, E) with or without 10 μM PP2, SRC-i-1, or gallein. (F) L929 cells were treated with sucrose (800 mM) and 10 μM PP2, SRC-i-1, or gallein. Cell lysates were analyzed by immunoblotting with anti-caveolin-1 and anti-phospho-caveolin-1 (Y14) antibodies. (G) L929 cells were treated with mTNF-α (10 ng·mL^{-1}) and zVAD (20 μM) with PP2 (10 μM) or an LCK inhibitor (7-cyclopentyl-5-(4-phenoxyphenyl)-7H-pyrrolo[2,3-d]pyrimidin-4-ylamine, 10 μM). Cell survival was measured with a Glo-ATP kit. (H) Wild-type and Fyn-knockout cells were challenged with mTNF-α (10 ng·mL^{-1}) and zVAD (20 μM). Cell viability was determined by CellTiter-Glo assay. ***$P < 0.001$, extremely significant; ns, $P \geq 0.05$, not significant.

inhibitory patterns when applied to cells expressing RIPK1-ΔDD (Fig. 2C), RIPK3 RHIM^{mut} (Fig. 2D), or MLKL (Fig. 2E). Gallein had little rescue effect on cell death in all these cell lines; SRC-i-1 partially attenuated cell death induced by RIPK1 oligomerization but not that induced by RIPK3 or MLKL oligomerization, whereas PP2 blocked cell death induced by the oligomerization of RIPK1 and RIPK3 but had no impact on MLKL-expressing cells. High osmolality (800 mM sucrose) induced the phosphorylation of caveolin-1 at Y14 through SRC [14]. Gallein, PP2, and SRC-i-1 all decreased the level of phospho-Cav1 (Y14), suggesting that these compounds efficiently inhibited SRC in L929 cells (Fig. 2F). Since SRC-i-1 functioned as an SRC inhibitor in L929 cells but had a negligible effect on cell death induced by the oligomerization of RIPK1, RIPK3, or MLKL, PP2 might function through a mechanism other than the inhibition of SRC.

PP2 was reported to have inhibitory effects on another Src family tyrosine kinase, Lck [15]. 7-Cyclopentyl-5-(4-phenoxyphenyl)-7H-pyrrolo[2,3-d]pyrimidin-4-ylamine [16], a more potent and selective Lck inhibitor than PP2, was tested, but the two inhibitors showed different effects (Fig. 2G). The loss of Fyn, another potential target of PP2 [17], did not block

necroptosis upon TNF-α and zVAD treatment (Fig. 2H). Taken together, these data suggest that PP2 blocks necroptosis by most likely directly inhibiting RIPK3 without participation of the Src family.

PP2 did not affect the autophosphorylation or kinase activity of RIPK3

Since both PP2 and GSK872 attenuated necroptosis but showed different abilities to induce apoptosis, the detailed molecular mechanism was further investigated. Using L929 cells carrying Flag-RIPK3, we first tested the integrity of the necrosome core, which consists of RIPK1, RIPK3, and MLKL. GSK872 disrupted the interaction between RIPK3 and MLKL but not that between RIPK3 and RIPK1, which is consistent with previous work [10,18]. However, PP2 did not impair the interaction between RIPK1 and RIPK3 or that between RIPK3 and MLKL (Fig. 3A). Moreover, while GSK872 largely impaired RIPK3 autophosphorylation at T231/S232 and the subsequent phosphorylation of MLKL, PP2 showed a negligible effect on RIPK3 autophosphorylation but largely diminished MLKL phosphorylation (Fig. 3B). A heterodimer system in RIPK3-deficient L929 cells generated by overexpressing RIPK3 RHIM mutants fused with FK506-binding protein (FKBP) or FRB* (a domain of mTOR with the point mutation T2098L) was further employed (Fig. 2B). Upon AP21967 stimulation, the two heterodimer adaptors, FKBP and FRB*, bound, thereby causing rapid necroptosis. The induced necroptosis could be significantly blocked by the addition of GSK872 or PP2 (Fig. 3C). Consistent with previous results, GSK872 blocked the phosphorylation of both RIPK3 and MLKL, while PP2 did not reduce the autophosphorylation of RIPK3 but depleted the phosphorylation of MLKL (Fig. 3D). Collectively, these data suggest that PP2 blocks necroptosis without affecting the phosphorylation status or kinase activity of RIPK3.

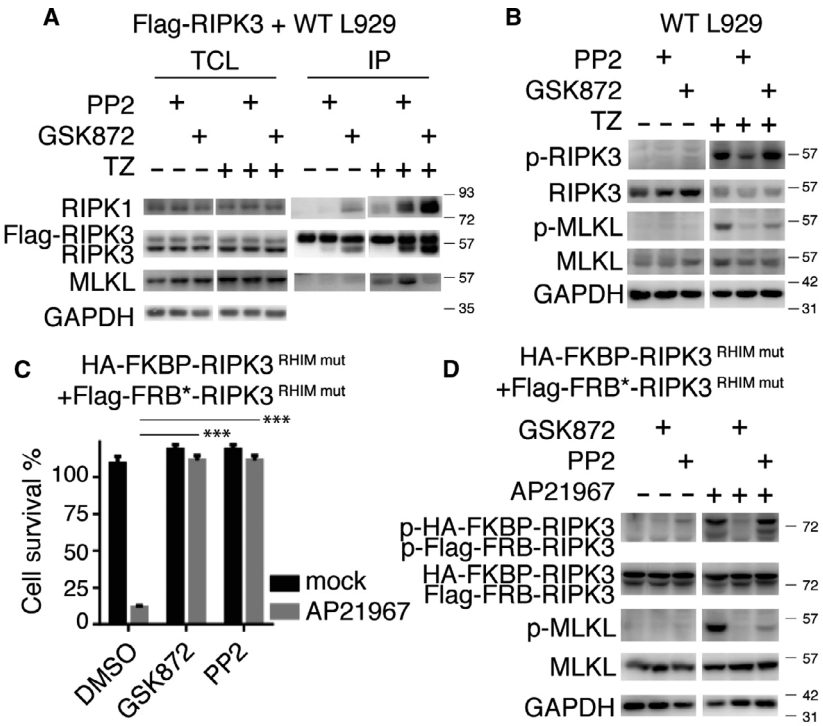

Fig. 3. PP2 does not impair RIPK3 autophosphorylation or MLKL recruitment. (A) Flag-RIPK3 epitope-expressing wild-type L929 cells were treated with TNF-α (10 ng·mL^{-1}), zVAD (20 μM), and PP2 (10 μM) or GSK872 (1 μM) as indicated. Cells were harvested for immunoprecipitation with anti-Flag beads and subjected to western blot analysis, and the indicated antibodies were then used to probe the necrosome proteins. IP, immunoprecipitation; TCL, total cell lysate. (B) WT L929 cells were also treated as described in (A), and total cellular lysates were analyzed by western blotting with anti-phospho-RIPK3 (T231/S232) and anti-phospho-MLKL (S345) antibodies. (C, D) RIPK3-knockout L929 cells overexpressing Flag-FRB*-RIPK3 and HA-FKBP-RIPK3 were treated with AP21967 (250 nM) for 4 h in (C) and 3 h in (D) with 10 μM PP2 or 1 μM GSK872. Cell viability was determined by CellTiter-Glo assay. (C). Cell lysates were subjected to western blotting with the indicated antibodies (D). Data from one experiment are representative of three independent experiments. ***$P < 0.001$, extremely significant; ns, $P \geq 0.05$, not significant.

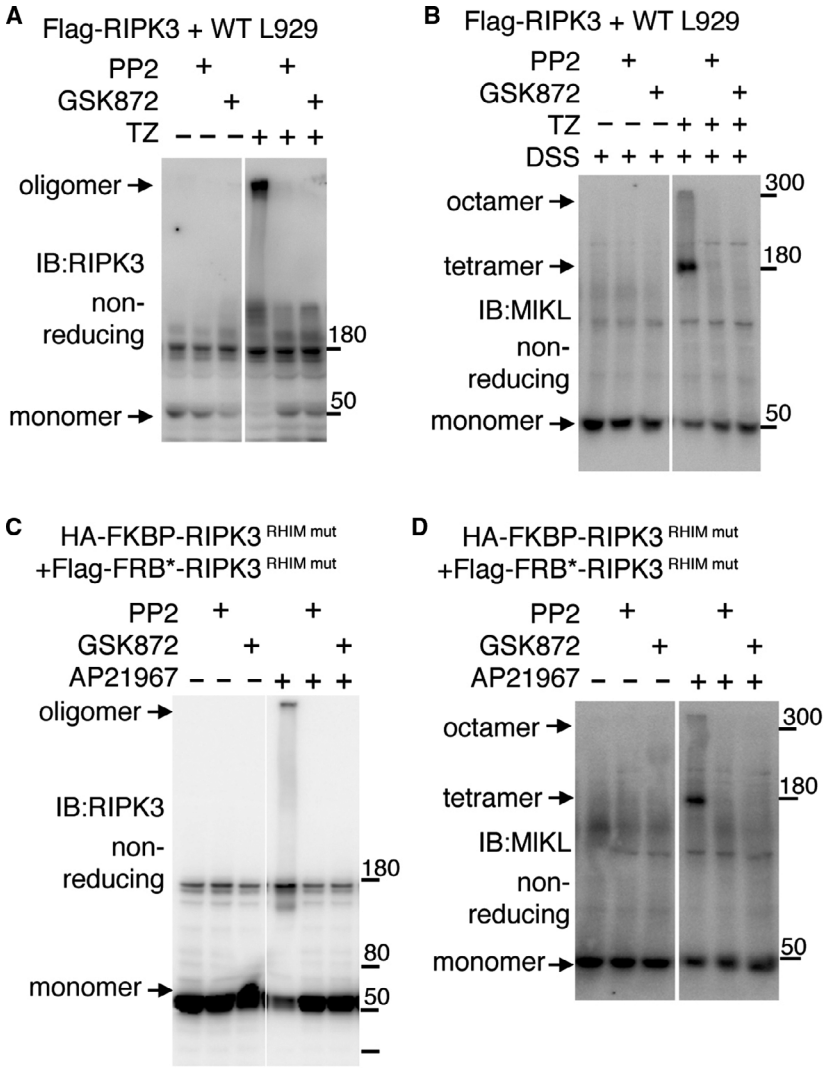

Fig. 4. PP2 blocks RIPK3 oligomerization. (A, B) Flag-RIPK3-expressing wild-type L929 cells were treated with TNF-α (10 ng·mL^{-1}) and zVAD (20 μM) with or without PP2 (10 μM)/GSK872 (1 μM) as indicated. Cell lysates were subjected to nonreducing SDS/PAGE and immunoblotting with anti-RIPK3 (A) and anti-MLKL (B) antibodies. (C, D) RIPK3-knockout L929 cells overexpressing Flag-FRB*-RIPK3 and HA-FKBP-RIPK3 were treated with AP21967, PP2 (10 μM), or GSK872 (1 μM) for 3 h. Cell lysates were subjected to nonreducing SDS/PAGE, followed by analysis with anti-RIPK3 (C) and anti-MLKL (D) antibodies. Data from one experiment are representative of three independent experiments.

PP2 disrupted the oligomerization of RIPK3

Next, we continued to investigate the oligomerization status of core necroptotic proteins, which is critical in necroptosis. RIPK1 and RIPK3 [19] were reported to form amyloid-like oligomers in necroptosis, while MLKL was shown to form disulfide bond-dependent tetramers and octamers resolved by nonreducing gel electrophoresis [20–22]. RIPK3 oligomers could be totally diminished by PP2 or GSK872 in WT L929 cell necroptosis induced by TZ (Fig. 4A), as were tetramers and octamers of MLKL (Fig. 4B). In FKBP- and FRB*-RIPK3-reconstituted L929 cells, RIPK3 dimers also tended to oligomerize into larger complexes, which could be totally blocked by GSK872 or PP2 (Fig. 4C). Tetramers and octamers of MLKL were also completely diminished upon treatment with GSK872 or PP2 (Fig. 4D). Together, these data indicate that PP2 blocks the oligomerization of RIPK3 to disrupt necroptosis.

Discussion

Necroptosis has been shown to play an important role in many inflammatory diseases, such as inflammatory bowel disease, intestinal inflammation [23], and atherosclerosis [2,24]. One of the main causes of necroptotic cell-induced inflammation is the release of cellular contents, including damage-associated molecular patterns, especially HMGB-1. RIPK3 has emerged as a central player in necroptosis and a potential target to control necroptosis-involved inflammatory diseases. In addition, RIPK3 can promote inflammatory responses independent of necroptotic cell death [25,26]. Recent studies using Mlkl−/− to exclude necroptosis

indicated that RIPK3 contributed to IL-1β production by activating the nucleotide-binding oligomerization domain-like receptor pyrin domain-containing 3 (NLRP3) inflammasome in arthritis mouse models [27] or endotoxic shock *in vivo* [28]. Thus, small-molecule inhibitors targeting RIPK3 hold great promise for therapeutic intervention in both necroptosis- and inflammasome-related inflammatory diseases. However, apoptotic cell death induced by RIPK3 kinase inhibitors represents a great challenge to the development of anti-inflammatory therapies targeting RIPK3. Herein, we found that PP2 blocked necroptosis without initiating apoptosis. A detailed mechanistic investigation revealed that PP2 directly inhibited the oligomerization of RIPK3 without affecting RIPK3 autophosphorylation. Thus, specific targeting of RIPK3 oligomerization may attenuate pathological necroptosis and inflammasome activation with reduced apoptotic side effects.

Protein oligomerization and polymerization play important roles in biological functions. For example, RIG1 and downstream MAVS form prion-like polymers that evoke an antiviral immune response [29,30]; the *Salmonella typhimurium* flagellin PrgJ activated the assembly of NAIP2 and NLRC4 into multisubunit disk-like structures to carry out a protective role in mouse models of colitis-associated colorectal cancer [31]. NLRP3, another example protein whose oligomerized form serves as a signal cascade platform, leads ASC to bridge caspase 1, forming ternary polymerization inflammasome complexes [32]. A recent example of RIPK3-mediated regulation of NLRP3 inflammasome activation comes from a lipopolysaccharide-induced acute lung injury mouse model [33]. In this study, we revealed that oligomerization of RIPK3 has critical functions in necroptosis. By utilizing a chemical-induced dimerization system, RIPK3 could form oligomers without other associated proteins to achieve autophosphorylation at T231/S232 and initiate necroptosis, suggesting that RIPK3 autophosphorylation at T231/S232 is essential but not sufficient for the activation of MLKL and that simultaneous oligomerization of RIPK3 is critically required. Unlike GSK872, PP2 blocked the oligomerization of RIPK3 without affecting RIPK3 autophosphorylation, thus preventing subsequent phosphorylation and oligomerization of MLKL and finally attenuating necroptosis without initiating RIPK3-dependent apoptosis. Taken together, our results suggest a new strategy to design an RIPK3 oligomerization blocker as a necroptosis and inflammasome inhibitor for therapeutic development.

Acknowledgements

The authors would like to thank Wanze Chen, Yaoji Liang, Deli Huang, and Jianfeng Wu for helpful discussions and suggestions, and Huaipeng Lin for help with data collection during revision. This work was supported by the National Key R&D Program (2017YFA0504504 and 2016YFA0502001), the National Natural Science Foundation of China (81661138005, 91853203, 81630042, 31500737, and 81603131), the China Postdoctoral Science Foundation (2016M600505 and 2017T100471), and the Fundamental Research Funds for the Central Universities of China (20720190101).

Author contributions

WL, HN, JH, LL, and XD designed the experiments, analyzed the data, and wrote the manuscripts. WL, HN, CC, and YL performed the cell biology experiment. SW, SH, and FG synthesized the chemical compounds. All authors provided comments and suggestions to the manuscripts.

References

1 Welz PS, Wullaert A, Vlantis K, Kondylis V, Fernandez-Majada V, Ermolaeva M, Kirsch P, Sterner-Kock A, van Loo G and Pasparakis M (2011) FADD prevents RIP3-mediated epithelial cell necrosis and chronic intestinal inflammation. *Nature* **477**, 330–334.

2 Lin J, Li H, Yang M, Ren J, Huang Z, Han F, Huang J, Ma J, Zhang D, Zhang Z *et al.* (2013) A role of RIP3-mediated macrophage necrosis in atherosclerosis development. *Cell Rep* **3**, 200–210.

3 Zhao H, Jaffer T, Eguchi S, Wang Z, Linkermann A and Ma D (2015) Role of necroptosis in the pathogenesis of solid organ injury. *Cell Death Dis* **6**, e1975.

4 Chen W, Zhou Z, Li L, Zhong CQ, Zheng X, Wu X, Zhang Y, Ma H, Huang D, Li W *et al.* (2013) Diverse sequence determinants control human and mouse receptor interacting protein 3 (RIP3) and mixed lineage kinase domain-like (MLKL) interaction in necroptotic signaling. *J Biol Chem* **288**, 16247–16261.

5 Rodriguez DA, Weinlich R, Brown S, Guy C, Fitzgerald P, Dillon CP, Oberst A, Quarato G, Low J, Cripps JG *et al.* (2016) Characterization of RIPK3-mediated phosphorylation of the activation loop of MLKL during necroptosis. *Cell Death Differ* **23**, 76–88.

6 Chen X, Li W, Ren J, Huang D, He WT, Song Y, Yang C, Li W, Zheng X, Chen P *et al.* (2014) Translocation of mixed lineage kinase domain-like

protein to plasma membrane leads to necrotic cell death. *Cell Res* **24**, 105–121.
7 Wang H, Sun L, Su L, Rizo J, Liu L, Wang LF, Wang FS and Wang X (2014) Mixed lineage kinase domain-like protein MLKL causes necrotic membrane disruption upon phosphorylation by RIP3. *Mol Cell* **54**, 133–146.
8 Huang D, Zheng X, Wang ZA, Chen X, He WT, Zhang Y, Xu JG, Zhao H, Shi W, Wang X *et al.* (2017) The MLKL channel in necroptosis is an octamer formed by tetramers in a dyadic process. *Mol Cell Biol* **37**, e00497-16.
9 Newton K, Dugger DL, Wickliffe KE, Kapoor N, de Almagro MC, Vucic D, Komuves L, Ferrando RE, French DM, Webster J *et al.* (2014) Activity of protein kinase RIPK3 determines whether cells die by necroptosis or apoptosis. *Science* **343**, 1357–1360.
10 Mandal P, Berger SB, Pillay S, Moriwaki K, Huang C, Guo H, Lich JD, Finger J, Kasparcova V, Votta B *et al.* (2014) RIP3 induces apoptosis independent of pronecrotic kinase activity. *Mol Cell* **56**, 481–495.
11 Zhang Y, Su SS, Zhao S, Yang Z, Zhong CQ, Chen X, Cai Q, Yang ZH, Huang D, Wu R *et al.* (2017) RIP1 autophosphorylation is promoted by mitochondrial ROS and is essential for RIP3 recruitment into necrosome. *Nat Commun* **8**, 14329.
12 Li L, Chen W, Liang Y, Ma H, Li W, Zhou Z, Li J, Ding Y, Ren J, Lin J *et al.* (2014) The Gbetagamma-Src signaling pathway regulates TNF-induced necroptosis via control of necrosome translocation. *Cell Res* **24**, 417–432.
13 Anastassiadis T, Deacon SW, Devarajan K, Ma H and Peterson JR (2011) Comprehensive assay of kinase catalytic activity reveals features of kinase inhibitor selectivity. *Nat Biotechnol* **29**, 1039.
14 Volonte D, Galbiati F, Pestell RG and Lisanti MP (2001) Cellular stress induces the tyrosine phosphorylation of caveolin-1 (Tyr(14)) via activation of p38 mitogen-activated protein kinase and c-Src kinase. Evidence for caveolae, the actin cytoskeleton, and focal adhesions as mechanical sensors of osmotic stress. *J Biol Chem* **276**, 8094–8103.
15 Giannini A and Bijlmakers M-J (2004) Regulation of the Src family kinase Lck by Hsp90 and ubiquitination. *Mol Cell Biol* **24**, 5667–5676.
16 Seo H-H, Kim SW, Lee CY, Lim KH, Lee J, Lim S, Lee S and Hwang K-C (2017) 7-cyclopentyl-5-(4-phenoxyphenyl)−7H-pyrrolo[2,3-d] pyrimidin-4-ylamine inhibits the proliferation and migration of vascular smooth muscle cells by suppressing ERK and Akt pathways. *Eur J Pharmacol* **798**, 35–42.
17 Hanke JH, Gardner JP, Dow RL, Changelian PS, Brissette WH, Weringer EJ, Pollok BA and Connelly PA (1996) Discovery of a novel, potent, and Src family-selective tyrosine kinase inhibitor: study of Lck- and FynT-dependent T cell activation. *J Biol Chem* **271**, 695–701.
18 Kaiser WJ, Sridharan H, Huang C, Mandal P, Upton JW, Gough PJ, Sehon CA, Marquis RW, Bertin J and Mocarski ES (2013) Toll-like receptor 3-mediated necrosis via TRIF, RIP3, and MLKL. *J Biol Chem* **288**, 31268–31279.
19 Li J, McQuade T, Siemer AB, Napetschnig J, Moriwaki K, Hsiao YS, Damko E, Moquin D, Walz T, McDermott A *et al.* (2012) The RIP1/RIP3 necrosome forms a functional amyloid signaling complex required for programmed necrosis. *Cell* **150**, 339–350.
20 Liu SZ, Liu H, Johnston A, Hanna-Addams S, Reynoso E, Xiang YG and Wang ZG (2017) MLKL forms disulfide bond-dependent amyloid-like polymers to induce necroptosis. *Proc Natl Acad Sci USA* **114**, E7450–E7459.
21 Dondelinger Y, Declercq W, Montessuit S, Roelandt R, Goncalves A, Bruggeman I, Hulpiau P, Weber K, Sehon CA, Marquis RW *et al.* (2014) MLKL compromises plasma membrane integrity by binding to phosphatidylinositol phosphates. *Cell Rep* **7**, 971–981.
22 Cai Z, Jitkaew S, Zhao J, Chiang HC, Choksi S, Liu J, Ward Y, Wu LG and Liu ZG (2014) Plasma membrane translocation of trimerized MLKL protein is required for TNF-induced necroptosis. *Nat Cell Biol* **16**, 55–65.
23 Pierdomenico M, Negroni A, Stronati L, Vitali R, Prete E, Bertin J, Gough PJ, Aloi M and Cucchiara S (2014) Necroptosis is active in children with inflammatory bowel disease and contributes to heighten intestinal inflammation. *Am J Gastroenterol* **109**, 279–287.
24 Tabas I (2010) Macrophage death and defective inflammation resolution in atherosclerosis. *Nat Rev Immunol* **10**, 36–46.
25 Moriwaki K and Chan FK (2016) Necroptosis-independent signaling by the RIP kinases in inflammation. *Cell Mol Life Sci* **73**, 2325–2334.
26 Moriwaki K and Chan FK (2017) The inflammatory signal adaptor RIPK3: functions beyond necroptosis. *Int Rev Cell Mol Biol* **328**, 253–275.
27 Lawlor KE, Khan N, Mildenhall A, Gerlic M, Croker BA, D'Cruz AA, Hall C, Kaur Spall S, Anderton H, Masters SL *et al.* (2015) RIPK3 promotes cell death and NLRP3 inflammasome activation in the absence of MLKL. *Nat Commun* **6**, 6282.
28 Wong WW, Vince JE, Lalaoui N, Lawlor KE, Chau D, Bankovacki A, Anderton H, Metcalf D, O'Reilly L, Jost PJ *et al.* (2014) cIAPs and XIAP regulate myelopoiesis through cytokine production in an RIPK1- and RIPK3-dependent manner. *Blood* **123**, 2562–2572.
29 Cai X, Chen J, Xu H, Liu S, Jiang QX, Halfmann R and Chen ZJ (2014) Prion-like polymerization underlies signal transduction in antiviral immune defense and inflammasome activation. *Cell* **156**, 1207–1222.

30 Hou F, Sun L, Zheng H, Skaug B, Jiang Q-X and Chen ZJ (2011) MAVS forms functional prion-like aggregates to activate and propagate antiviral innate immune response. *Cell* **146**, 448–461.
31 Zhang L, Chen S, Ruan J, Wu J, Tong AB, Yin Q, Li Y, David L, Lu A, Wang WL *et al.* (2015) Cryo-EM structure of the activated NAIP2-NLRC4 inflammasome reveals nucleated polymerization. *Science* **350**, 404–409.
32 Lu A, Magupalli VG, Ruan J, Yin Q, Atianand MK, Vos MR, Schröder GF, Fitzgerald KA, Wu H and Egelman EH (2014) Unified polymerization mechanism for the assembly of ASC-dependent inflammasomes. *Cell* **156**, 1193–1206.
33 Chen J, Wang S, Fu R, Zhou M, Zhang T, Pan W, Yang N and Huang Y (2018) RIP3 dependent NLRP3 inflammasome activation is implicated in acute lung injury in mice. *J Transl Med* **16**, 233.